Does complex mean accurate: comparing COVID-19 propagation models with different structural complexity ⋆

Israel Huaman[0000−0003−4677−8259] and Vasiliy Leonenko[0000−0001−7070−6584]

ITMO University, 49 Kronverksky Pr., St. Petersburg, Russia 197101

Abstract. During the last years, a wide variety of epidemic models was employed to analyze the spread of COVID-19. Finding the most suitable model according to the available epidemic data is an important task to consider. In this project, we perform a comparison of several models of COVID-19 dynamics and analyze the dependence of their accuracy on their structural complexity, using COVID-19 incidence data for St. Petersburg. The assessment is based on Akaike information criterion (AIC). The results of the study contribute to understanding how to properly choose the complexity of an explanatory model for a given epidemic dataset.

Keywords: mathematical modeling · epidemiology · COVID-19 · structural complexity · logistic regression · compartmental models · Akaike information criterion

1 Introduction

During the last years, a wide variety of epidemic models was employed to analyze the spread of COVID-19. As a rule, the modeling aim is to assess the impact of the epidemics and the efficiency of control measures to reduce the social and economic toll. In this regard, finding the most suitable model according to the available epidemic data is an important task to consider. The most common methodologies used for COVID-19 modeling include classical compartmental SEIR models based on difference and differential equations [1–4], metapopulation models which simulate population migration between countries and cities [5, 6], and multi-agent models [7] which are beneficial in simulating outbreaks in high detail. In the majority of the investigations, the choice of an optimal model structure suitable for the task is not discussed and there is no opportunity to compare the accuracy of different models calibrated to a fixed dataset. At the same time, it is known that the selected model type affects the modeling outcome, and, consequentially, the choice of the most effective control measures [17]. Particularly, due to remaining blind spots regarding COVID-19 incidence dynamics, simpler models may have an advantage over more complicated ones, because the output of the latter might demonstrate higher levels of uncertainty.

⋆ This research was supported by The Russian Science Foundation, Agreement #22-71-10067

ICCS Camera Ready Version 2023
To cite this paper please use the final published version:
DOI: 10.1007/978-3-031-36024-4_21

In this study, following the logic of our earlier research [13], we perform a retrospective analysis of COVID-19 dynamics using a family of models based on distinct modeling approaches. Several types of logistic models and SEIR compartmental models are calibrated to COVID-19 data, with the disease incidence in St. Petersburg in 2020-2022 used as a test dataset, and their accuracy is compared using the modification of the indicator based on Akaike information criterion [16], namely, AICc [17]. We demonstrate the resulting goodness of fit of the models and discuss how to find a best compromise between the model complexity and model calibration accuracy for a given dataset. Since COVID-19 modeling research mostly inherit the methods from earlier works in mathematical epidemiology, particularly, dedicated to influenza modeling (e.g., [9], [12]), the described methodology can be easily generalized to be used for any epidemic ARIs.

2 Methods

The data for model calibration was taken from the repository [18] which contains daily dynamics of COVID-19 in St. Petersburg, Russia. At the time of our study, the sample contained disease data from 02-03-2020 to 15-12-2022. The following datasets were formed for analysis:

- Daily incidence, i.e. number of active cases — taken directly from the source data;
- Total cumulative number of registered cases — calculated from the source data.

The whole dataset ('Multiwave') was also split into six separate outbreaks of COVID-19 ('Waves') according to the information available from open sources. The following model types were compared:

- Models based on the logistic equations: a single equation for separate COVID waves and a sum of logistic equations for the multiwave epidemic;
- Compartmental differential SEIR models similar to those used by the authors for influenza prediction [8], in two modifications: for single COVID waves (constant intensity of infection) and the multiwave epidemic (variable intensity of infection).

The description of the models follows.

2.1 Logistic models

The single-wave model calibrated to the total number of registered cases is based on the logistic model [14] and has the following form:

$$\frac{dC}{dt} = rC\left(1 - \frac{C}{K}\right), \; C(0) = C_0 \geq 0,$$

ICCS Camera Ready Version 2023
To cite this paper please use the final published version:
DOI: 10.1007/978-3-031-36024-4_21

where C is the total number of registered cases of COVID-19, t is the current time, r is the infection propagation intensity and K is the maximum load, which is equal to the maximal possible number of infection cases. We use the $optimize.fmin$ function from Python *scipy* library to find the optimal values for r and K. Fig. 1a demonstrates the calibration result for the second wave of COVID-19. With the help of some simple arithmetic operations, this model can also produce output in a form of daily incidence, which makes it possible to use daily incidence data for model calibration (Fig. 1b).

To describe a whole period of available COVID-19 epidemic data, corresponding to a multiwave epidemic, a multiwave logistic model was build according to the approach proposed in [15]. This model is comprised of a sum of several logistic equations, each of them reflecting the introduction of a new COVID wave. The fitted model trajectory is shown in Fig. 1c. Similarly to the single-wave case, the modeling output can be recalculated to obtain simulated daily incidence. The resulting modeling curve calibrated to data is shown in Fig. 1d.

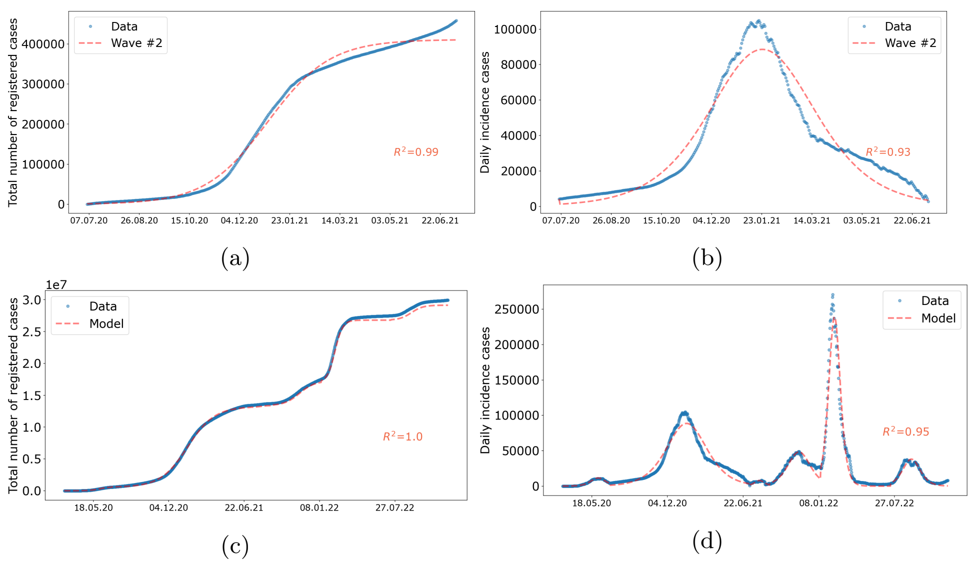

Fig. 1: Fitted logistic models: (a) single-wave, total number of registered cases; (b) single-wave, daily incidence; (c) multiwave, total number of registered cases; (d) multiwave, daily incidence data.

It is worth mentioning that the multiwave model in the described form generates a 'smooth' (i.e. differentiable) curve which worsens the fit quality of late COVID waves. In Fig. 1c it can be seen that the model trajectory starting approximately from April, 2022 is lower than the data. To fix this problem and thus enhance the fit quality, we present an additional 'adjusted' multiwave logistic model. In this model, the initial position of each simulated wave is artificially

ICCS Camera Ready Version 2023
To cite this paper please use the final published version:
DOI: 10.1007/978-3-031-36024-4_21

matched to the corresponding point in the dataset point of each single wave (thus, simulated incidence in the first day of each COVID wave is equal to the real incidence). The resulting simulated function is non-differentiable in the points of change of COVID waves.

2.2 SEIR models

The compartmental SEIR model can be expressed as a system of ordinary differential equations in the following form:

$$\begin{aligned}
&\frac{dS(t)}{dt} = -\beta S(t)I(t) + \epsilon R(t);\\
&\frac{dE(t)}{dt} = \beta S(t)I(t) - \gamma E(t);\\
&\frac{dI(t)}{dt} = \gamma E(t) - \delta I(t);\\
&\frac{dR(t)}{dt} = \delta I(t) - \epsilon R(t),\\
&S(t_0) = S^{(0)} \geq 0, E(t_0) = E^{(0)} \geq 0, I(t_0) = I^{(0)} \geq 0;\\
&S^{(0)} + E^{(0)} + I^{(0)} = \alpha \in [0;1], R(t_0) = 1 - \alpha,
\end{aligned}$$

where $S(t)$ is the proportion of susceptible individuals in the population at time t, $E(t)$ is the proportion of individuals in incubation period at time t, $I(t)$ is the proportion of infected individuals at a given time t, $R(t)$ is the proportion of recovered individuals at the time t, α is the initial proportion of susceptible individuals in the population, δ is the recovery rate of infected individuals, γ is the intensity of transition to the stage of infected individuals, ϵ is the percentage of recovered population that will become susceptible again and β is the coefficient of intensity of effective contacts of individuals (i.e. contacts with subsequent infection).

For a single wave case (Fig. 2a), we consider the intensity β a constant. In a multiwave case, the intensity is a function of time, i.e. $\beta = \beta(t)$. This modification reflects the influence of introduced control measures on intensity of contacts, as well as the influence of change in circulating SARS-CoV-2 virus strains on disease infectivity. In the current research, we used a piece-wise constant $\beta(t)$. The time moments corresponding to the days when the intensity of contacts in St. Petersburg might have changed were selected from the portal of the Government of St. Petersburg where reports on initiated control measures were published [20]. Initially, 38 dates were selected. Several events corresponding to close dates were combined, which resulted in 35 potential moments of changes in the intensity of contacts. Each moment was assigned a characteristic that assumes the direction of changes in intensity (the number of contacts decreases with increasing restrictions on disease control and increases with their weakening), as well as a subjective categorical assessment of the possible strength of the impact of the corresponding event on the epidemic dynamics. Using this information, we defined the moments of change of $\beta(t)$, splitted the incidence dataset into subsets

ICCS Camera Ready Version 2023
To cite this paper please use the final published version:
DOI: 10.1007/978-3-031-36024-4_21

corresponding to each of the values of intensity β_i (see Fig. 2b) and found those values by sequentially optimizing the model on each of the incidence subsets separately.

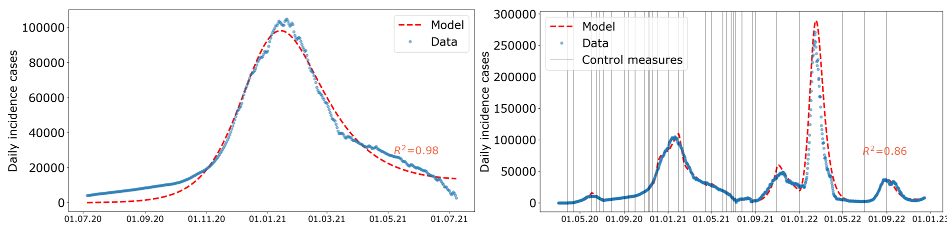

(a) (b)

Fig. 2: SEIR models calibrated to daily incidence data: (a) single-wave case; (b) multiwave case.

2.3 Accuracy indicators

Our main indicator for model comparison is Akaike information criterion (AIC) for models calibrated with the least square method, in its corrected version $AICc$ which is more suitable for small samples ($k > n/40$):

$$AICc = n \ln(RSS) + 2k + \frac{2k^2 + 2k}{n - k - 1},$$

where RSS is the residual sum of squares, k is the number of free parameters and n is the data sample size. As an auxiliary indicator, which is not dependent on model complexity (i.e. the number of free parameters k), we employed the coefficient of determination R^2:

$$R^2 = 1 - \frac{RSS}{TSS},$$

where TSS is total sum of squares (the explained sum of squares plus the residual sum of squares).

3 Results

The calibration speed for different models is shown in Table 1. It is noticeable that calibration algorithms for logistic models are approximately twice faster than those for SEIR models, which could be important for experiments with numerous calibration runs, such as calibrating a multitude of datasets or sensitivity analysis. The results of comparison of accuracy are demonstrated in Tables 2 – 4. As Table 2 demonstrates, the logistic model fitted to incidence data presented

ICCS Camera Ready Version 2023
To cite this paper please use the final published version:
DOI: 10.1007/978-3-031-36024-4_21

the lower AIC value for multiwave case[1]. In case of model fitting to separate waves, the SEIR model almost always demonstrated the lowest AIC value, except for wave 5. At the same time, according to Table 3, logistic models fitted to total cases have the highest R^2 values, including a maximum score of 1.0 obtained on multiwave data. However, single-wave SEIR models present higher R^2 values in most of the cases compared to logistic models fitted to the same data format (daily incidence). Table 4 demonstrates that an adjusted logistic model is slightly better by its AIC than the original logistic multiwave model which generates differentiable simulated curve.

Table 1: Execution time for different models

Model	Multiwave	Wave 1	Wave 2	Wave 3	Wave 4	Wave 5	Wave 6
Logistic, total cases	2.11	0.70	0.87	0.71	0.68	0.74	0.74
Logistic, incidence	2.33	0.70	0.80	0.69	0.65	0.74	0.71
SEIR	5.72	1.48	2.63	0.63	1.55	0.73	1.84

Table 2: *AIC* for incidence models (best calibration in bold)

Model	Multiwave	Wave 1	Wave 2	Wave 3	Wave 4	Wave 5	Wave 6
Logistic	$\mathbf{1.75 \cdot 10^7}$	$0.47 \cdot 10^7$	$1.55 \cdot 10^7$	$0.65 \cdot 10^7$	$1.28 \cdot 10^7$	$\mathbf{1.68 \cdot 10^7}$	$1.17 \cdot 10^7$
SEIR	$5.24 \cdot 10^7$	$\mathbf{0.35 \cdot 10^7}$	$\mathbf{1.38 \cdot 10^7}$	$\mathbf{0.61 \cdot 10^7}$	$\mathbf{0.91 \cdot 10^7}$	$1.91 \cdot 10^7$	$\mathbf{1.05 \cdot 10^7}$

Table 3: R^2 for all models (best calibration in bold)

Model	Multiwave	Wave 1	Wave 2	Wave 3	Wave 4	Wave 5	Wave 6
Logistic, total cases	**1.0**	**0.99**	**0.99**	**0.99**	**1.0**	**0.99**	**0.90**
Logistic, incidence	0.95	**0.99**	0.93	0.46	0.79	0.95	**0.90**
SEIR	0.86	0.99	0.98	0.58	0.98	0.8	0.95

Table 4: Calibration accuracy of multiwave logistic models

Indicator	AIC	R^2
Original	$2.96 \cdot 10^7$	1.0
Adjusted	$\mathbf{2.64 \cdot 10^7}$	1.0

4 Discussion

In this study, we showed how accuracy of the model fit could be compared accounting for their structural complexity. The selection of the winning model could depend on data representation (daily incidence vs total registered cases), the period of regarded data (one wave vs multiwave) and, last but not least, the desired output indicators. It is demonstrated that comparing models solely by the quality of fit (R^2 in our case) may be misleading, which becomes clear by

[1] Since *AIC* can be compared only for the models fitted to the same data, in Table 2 we do not demonstrate results for logistic model calibrated to total cases.

ICCS Camera Ready Version 2023
To cite this paper please use the final published version:
DOI: 10.1007/978-3-031-36024-4_21

looking at Tables 3 and 4. According to the values of AIC, SEIR models should be preferred in case of analysing single COVID-19 waves. At the same time, while regarding multiwave disease dynamics, a multiwave SEIR model loses to logistic models because of its increased number of parameters. Thus, we can conclude that in some cases complex indeed does not mean accurate.

It is important to mention that the comparison of models solely based on AIC cannot be regarded as exhaustive, because many aspects might be missing in this case. First of all, unlike R^2, AIC is calculated in absolute values and thus is dependent on the data representation. Particularly, the direct comparison of AIC for the logistic model calibrated to total cases number and the same model calibrated to incidence data is impossible, whereas we can compare them via R^2. Also, some important epidemic indicators which could be provided by one model type are unavailable in another model type. For instance, logistic models are unable to deliver the value of basic reproduction number R_0 [19] because the recovery process in such models is entirely omitted. This aspect can be crucial for epidemiologists, since this parameter is informative when a particular outbreak is studied. Regarding the assessment of the cost-effectiveness of control measures, multiwave models subjectively seem to be more efficient because they allow to replicate the whole process instead of separating it into parts like in single-wave models. When talking about incidence prediction, which is another meaningful task for the models, the application of the mentioned models might differ in efficiency. The authors believe that logistic models will give a smoother trend thus reducing variation in error sample, although they potentially give a biased solution. In their turn, SEIR models due to bigger number of parameters might demonstrate larger confidence intervals for the predicted incidence. In another words, fitting SEIR multiwave models to incomplete incidence data could be challenging due to the greater variability of the output. In the forthcoming studies, we plan to explicitly quantify our hypotheses related to applicability of the models for assessing epidemic indicators (including incidence forecasting with uncertainty assessment). Also, an important research aim is to generalize the proposed methods and algorithms to make them suitable for the other model types, including multiagent models [10], [11].

References

1. Read, J. et al. Novel coronavirus 2019-nCoV (COVID-19): early estimation of epidemiological parameters and epidemic size estimates. *Philosophical Transactions Of The Royal Society B*. **376**, 20200265 (2021)
2. Maier, B. & Brockmann, D. Effective containment explains subexponential growth in recent confirmed COVID-19 cases in China. *Science*. **368**, 742-746 (2020)
3. Iboi, E. et al. Mathematical modeling and analysis of COVID-19 pandemic in Nigeria. *Mathematical Biosciences And Engineering*. **17**, 7192-7220 (2020)
4. López, L. & Rodo, X. A modified SEIR model to predict the COVID-19 outbreak in Spain and Italy: simulating control scenarios and multi-scale epidemics. *Results In Physics*. **21** pp. 103746 (2021)
5. Chinazzi, M. et al. The effect of travel restrictions on the spread of the 2019 novel coronavirus (COVID-19) outbreak. *Science*. **368**, 395-400 (2020)

ICCS Camera Ready Version 2023
To cite this paper please use the final published version:
DOI: 10.1007/978-3-031-36024-4_21

6. Bajardi, P. et al. Human mobility networks, travel restrictions, and the global spread of 2009 H1N1 pandemic. *PloS One*. **6**, e16591 (2011)
7. Hoertel, N. et al. Facing the COVID-19 epidemic in NYC: a stochastic agent-based model of various intervention strategies. *MedRxiv*. (2020)
8. Leonenko, V. N., Ivanov, S. V. Prediction of influenza peaks in Russian cities: Comparing the accuracy of two SEIR models. *Mathematical Biosciences & Engineering*. **15(1)**, 209 (2018).
9. Leonenko, V., Bobashev G. Analyzing influenza outbreaks in Russia using an age-structured dynamic transmission model. *Epidemics*. **29**, 100358 (2019)
10. Leonenko V., Lobachev A., Bobashev G. Spatial modeling of influenza outbreaks in Saint Petersburg using synthetic populations. *Computational Science–ICCS 2019: 19th International Conference, Faro, Portugal, June 12–14, 2019, Proceedings, Part I* **19** 492-505 (2019)
11. Leonenko V., Arzamastsev S., Bobashev G. Contact patterns and influenza outbreaks in Russian cities: A proof-of-concept study via agent-based modeling. *Journal of Computational Science*. **44**, 101156 (2020)
12. Leonenko, V. Herd immunity levels and multi-strain influenza epidemics in Russia: a modelling study. *Russian Journal Of Numerical Analysis And Mathematical Modelling*. **36**, 279-291 (2021)
13. Huaman, I., Plesovskaya, E. & Leonenko, V. Matching model complexity with data detail: influenza propagation modeling as a case study. *2022 IEEE International Multi-Conference On Engineering, Computer And Information Sciences (SIBIRCON)*. pp. 650-654 (2022)
14. Yang, W. et al. Rational evaluation of various epidemic models based on the COVID-19 data of China. *Epidemics*. **37** pp. 100501 (2021)
15. Kurkina, E. & Koltsova, E. Mathematical modeling of the propagation of Covid-19 pandemic waves in the World. *Computational Mathematics And Modeling*. **32** pp. 147-170 (2021)
16. Roda, W., Varughese, M., Han, D. & Li, M. Why is it difficult to accurately predict the COVID-19 epidemic?. *Infectious Disease Modelling*. **5** pp. 271-281 (2020)
17. Mathieu, J. et al. Tactical robust decision-making methodology: Effect of disease spread model fidelity on option awareness.. *ISCRAM*. (2010)
18. Kouprianov, A. Monitoring COVID-19 epidemic in St. Petersburg, Russia: Data and scripts (2021), https://github.com/alexei-kouprianov/COVID-19.SPb.monitoring
19. Harko, T., Lobo, F. & Mak, M. Exact analytical solutions of the Susceptible-Infected-Recovered (SIR) epidemic model and of the SIR model with equal death and birth rates. *Applied Mathematics And Computation*. **236** pp. 184-194 (2014)
20. "St Petersburg against the coronavirus. Official Information." (In Russian). URL: https://www.gov.spb.ru/covid-19/dokument/

ICCS Camera Ready Version 2023
To cite this paper please use the final published version:
DOI: 10.1007/978-3-031-36024-4_21